STAR Protocols

CellPress
OPEN ACCESS

Protocol

# Protocol to construct biomimetic carbon fiber composites with improved interfacial strength

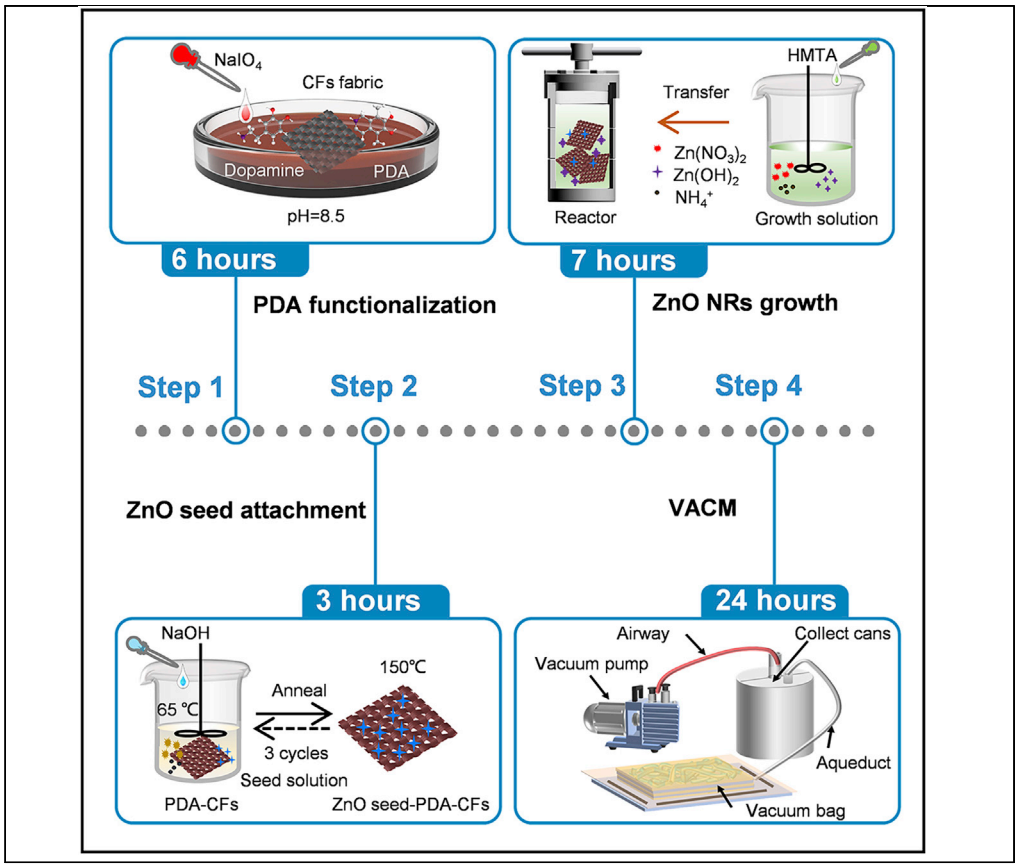


Weak interfacial strength restricts the mechanical properties of carbon fiber-reinforced composites. Here, inspired by natural hook-groove microstructure system (HGMS) of black kite (*Milvus migrans*), we detail the steps to construct a biomimetic HGMS based on dopamine-functionalized carbon fibers (CFs) and zinc oxide nanorods (ZnO NRs) using a two-step modification approach. We describe the fabrication of biomimetic carbon fiber composites using vacuum-assisted contact molding (VACM) and subsequent characterization using standard comprehensive mechanical tests techniques.

Publisher's note: Undertaking any experimental protocol requires adherence to local institutional guidelines for laboratory safety and ethics.

Yufei Wang, Zhengzhi Mu, Zhiyan Zhang, Wenda Song, Ze Wang, Zhiwu Han, Luquan Ren

zmu@jlu.edu.cn (Z.M.)
zwhan@jlu.edu.cn (Z.H.)

## Highlights

Investigation of natural HGMS and mechanical interlocking mechanism

Steps to build a biomimetic HGMS based on functionalized CFs and ZnO NRs

Vacuum-assisted contact molding used to fabricate biomimetic carbon fiber composites

Guidance for mechanical performance test of the bioinspired CFRCs

Wang et al., STAR Protocols 3, 101805
December 16, 2022 
https://doi.org/10.1016/j.xpro.2022.101805

STAR Protocols

CellPress
OPEN ACCESS

Protocol

# Protocol to construct biomimetic carbon fiber composites with improved interfacial strength

Yufei Wang,[1] Zhengzhi Mu,[1,2,3,5,*] Zhiyan Zhang,[1] Wenda Song,[1] Ze Wang,[1,2,3] Zhiwu Han,[1,3,4,*] and Luquan Ren[1,3]

[1]Key Laboratory of Bionic Engineering, Ministry of Education, Jilin University, Changchun 130022, China

[2]School of Mechanical and Aerospace Engineering, Jilin University, Changchun 130022, China

[3]Weihai Institute for Bionics, Jilin University, Weihai 264200, China

[4]Technical contact

[5]Lead contact

*Correspondence: zmu@jlu.edu.cn (Z.M.), zwhan@jlu.edu.cn (Z.H.)
https://doi.org/10.1016/j.xpro.2022.101805

## SUMMARY

**Weak interfacial strength restricts the mechanical properties of carbon fiber-reinforced composites. Here, inspired by natural hook-groove microstructure system (HGMS) of black kite (*Milvus migrans*), we detail the steps to construct a biomimetic HGMS based on dopamine-functionalized carbon fibers (CFs) and zinc oxide nanorods (ZnO NRs) using a two-step modification approach. We describe the fabrication of biomimetic carbon fiber composites using vacuum-assisted contact molding (VACM) and subsequent characterization using standard comprehensive mechanical tests techniques.**

**For complete details on the use and execution of this protocol, please refer to Wang et al. (2022).**

## BEFORE YOU BEGIN

Refer to "materials and equipment" for a list of equipment needed for this protocol.

### Characterization and interlocking mechanism of natural HGMS

Timing: 1–2 h

1. Interlocking structure characterization of natural HGMS.
   a. Place the intact feather in a glass container with a diameter of more than 400 mm and soak into ethanol solution (99.7%, Shanghai Aladdin Biochemical Technology Co., Ltd., China) for 10–15 min.
   b. Then apply ultrasonic cleaning (KS-800KDE, Kunshan Jielimei Ultrasonic Instrument Co., Ltd., China) for 5–8 min (220 V, 40 KHz, 25°C) to remove tiny impurities on the feather surface.
   c. Volatize the residual ethanol solution on the feather surface and dry naturally at room temperature (25°C).
   d. Cut off a piece of feather vane off along the feather shaft (Figures 1A and 1B).
   e. Spray the feather vane sample with a thin layer of Au nanoparticles (NPs) for 30 min using vacuum ion sputtering apparatus (Q150RS).
   f. Perform SEM (JSM-6700F, JEOL) observation to obtain the digital images of micro/nanoscale structures of feather vane sample (Figures 1C and 1D).
2. Interlocking mechanism observation of natural HGMS.

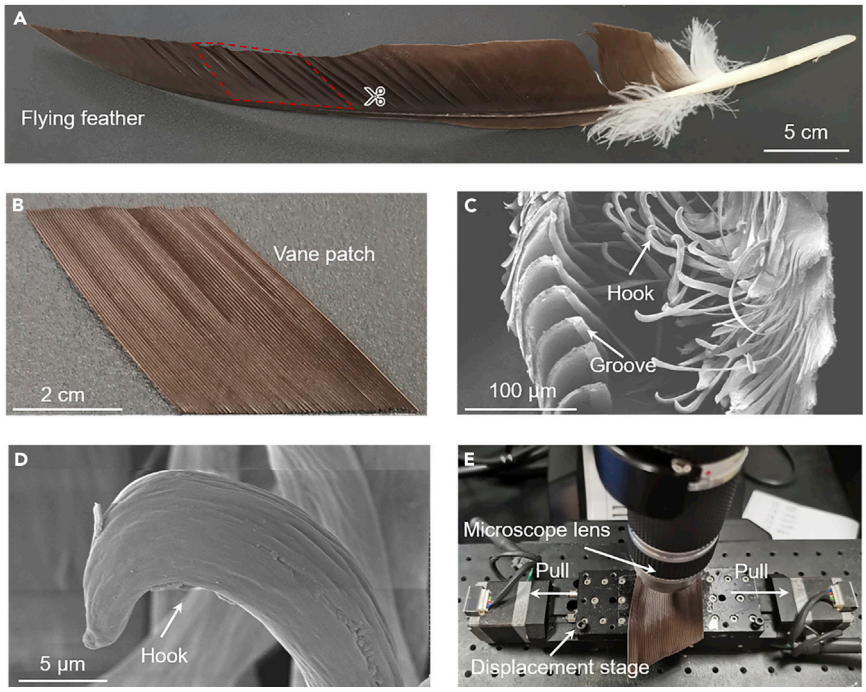


**Figure 1. Selected feather vane and testing device for interlocking mechanism revelation**

(A) An intact flying feather of Black Kite (*Milvus migrans*).

(B) A digital photo of the selected feather vane patch.

(C) Interlocking structures between microscale hooks and grooves.

(D) A single hook structure.

(E) A setup of the testing device for dynamic interlocking behavior observation.

a. Apply glue (Ergo 5400, Ergo Workshop, China) to paste both ends of the feather vane sample on the displacement stage (SURUGA SEIKI, Japan).

***Note:*** This aims at ensuring the direction of barb arrangement is always consistent with the movement direction of the displacement stage.

b. Place the displacement stage with feather vane sample stably under the lens of a stereoscopic microscope (VHX-S650E).

***Note:*** To obtain a clear observation vision, the microscope lens should be adjusted to an appropriate distance (5–15 mm) between lens and sample.

c. Control cycled separation and recovery of natural HGMS by the movement of the displacement stage (0.5 mm/s) (Figure 1E).

d. Observe and record dynamic interlocking behaviors in real time using the microscope (Figure 2).

## KEY RESOURCES TABLE

| REAGENT or RESOURCE | SOURCE | IDENTIFIER |
|---|---|---|
| Chemicals, peptides, and recombinant proteins | | |
| Epoxy resin (E-51) AB adhesives | Kunshan Eituo Composites Co., Ltd., China | N/A |
| JSM-519 resin release agent | Kunshan Eituo Composites Co., Ltd., China | N/A |

(*Continued on next page*)

| *Continued* | | |
|---|---|---|
| REAGENT or RESOURCE | SOURCE | IDENTIFIER |
| Glue (Ergo 5400) | Ergo Workshop, China | N/A |
| Acetone | Shanghai Aladdin Biochemical Technology Co., Ltd., China | CAS: 15364-56-4 |
| NaOH | Shanghai Aladdin Biochemical Technology Co., Ltd., China | CAS: 1310-73-2 |
| Ethanol | Shanghai Aladdin Biochemical Technology Co., Ltd., China | CAS: 64-17-5 |
| $Zn(CH_3COO)_2 \cdot 2H_2O$, 99.0% | Shanghai Aladdin Biochemical Technology Co., Ltd., China | CAS: 5970-45-6 |
| Dopamine hydrochloride, 98.0% | Shanghai Aladdin Biochemical Technology Co., Ltd., China | CAS: 51-61-6 |
| TRIS, 99.0% | Shanghai Aladdin Biochemical Technology Co., Ltd., China | CAS: 77-86-1 |
| Sodium periodate | Shanghai Aladdin Biochemical Technology Co., Ltd., China | CAS: 7790-28-5 |
| $Zn(NO_3)_2 \cdot 6H_2O$, 99.0% | Shanghai Aladdin Biochemical Technology Co., Ltd., China | CAS: 10198-18-6 |
| HMTA, 99.0% | Shanghai Aladdin Biochemical Technology Co., Ltd., China | CAS: 100-97-0 |
| Biological samples | | |
| Feathers of Black Kite | Qiusheng Feather Workshop, China | https://m.tb.cn/h.fmqYLw0?tk=oK4s2f07bme |
| Other | | |
| T300 CFs | Toray Ltd., Japan | N/A |
| Vacuum bag | Kunshan Eituo Composites Co., Ltd., China | N/A |
| Adhesive felt | Kunshan Eituo Composites Co., Ltd., China | N/A |
| Isolation film | Kunshan Eituo Composites Co., Ltd., China | N/A |
| Oven | Tianjin St Instrument Co., Ltd., China | 101-2AB |
| Analytical balance | Sartorius, Germany | BSA224S |
| Vacuum pump | Tengyuan Workshop, China | 550D |
| Ultrasonic machine | Kunshan Jielimei Ultrasonic Instrument Co., Ltd., China | KS-800KDE |
| Displacement stage | SURUGA SEIKI, Japan | BSS16-40A |
| Stereoscopic microscope | KEYENCE, Japan | VHX-S650E |
| Scanning electron microscope (SEM) | JEOL, Japan | JSM-6700F |
| Fourier transform infrared spectroscope (FTIR) | Shimadzu, Japan | IRAffinity-1S-WL |
| Energy-dispersive spectroscope (EDS) | Oxford Instruments, UK | Oxford X-MaxN 150 |
| X-ray diffraction (XRD) | Rigaku, Japan | Smartlab Sex-Ray generator 3 kW closed tube |
| Ion sputtering apparatus | Quorum, UK | Q150RS |
| Electrohydraulic universal testing machine | MTS, USA | MTS 810 |

## MATERIALS AND EQUIPMENT

| **Poly dopamine (PDA) solution** | | |
|---|---|---|
| Reagent | Final concentration | Amount |
| TRIS | N/A | 0.60 g |
| Dopamine hydrochloride | 1 g/L | 0.50 g |
| $NaIO_4$ | N/A | 2.26 g |
| $ddH_2O$ | N/A | 500 mL |
| **Total** | **N/A** | **500 mL** |

*Note:* The PDA solution should be freshly made and stored at 4°C before use. Its final pH should be 8.5.

| **ZnO seed solution** | | |
|---|---|---|
| Reagent | Final concentration | Amount |
| NaOH | 20 mM | 0.80 g |
| $Zn(CH_3COO)_2 \cdot 2H_2O$ | 12.50 mM | 2.74 g |
| EtOH | N/A | 800 mL |
| **Total** | **N/A** | **800 mL** |

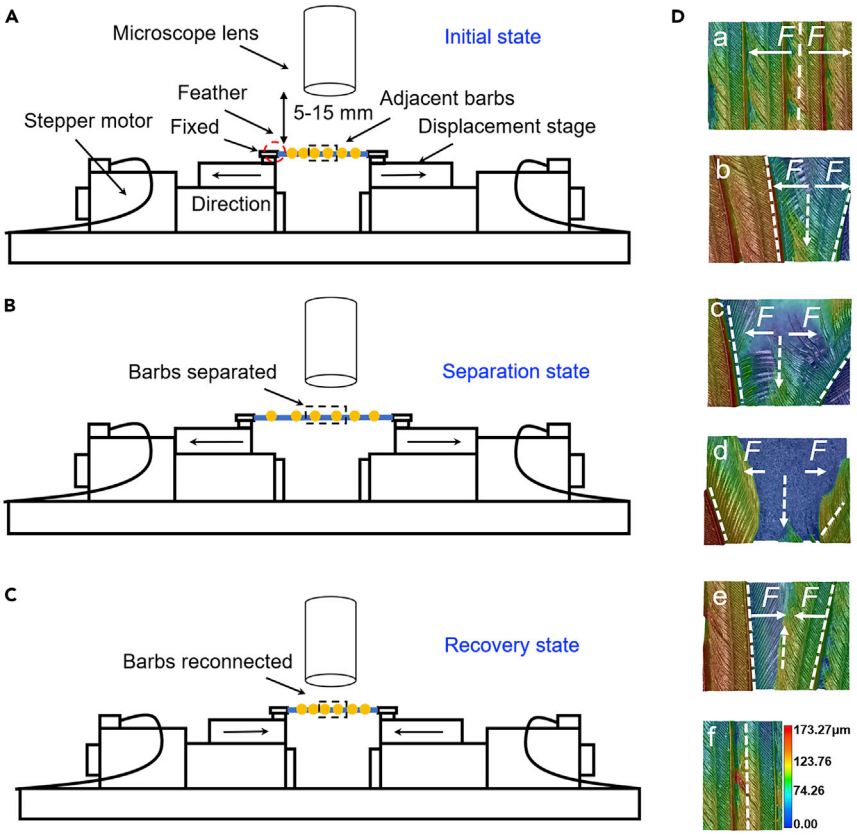


**Figure 2. Diagram of the testing device for dynamic interlocking behavior observation**

(A) Initial state.

(B) Separation state.

(C) Recovery state.

(D) A image sequence (a–f) of the separation-recovery cycle of adjacent barbs with natural HGMS.

*Note:* The seed solution should be cooled by ice bath as soon as possible to prevent excessive crystallization of ZnO. It should be freshly made and stored at 4°C before use.

| **ZnO growth solution** | | |
|---|---|---|
| Reagent | Final concentration | Amount |
| HMTA | 20 mM | 7.4373 g |
| $Zn(NO_3)_2 \cdot 6H_2O$ | 11.78 mM | 3.5048 g |
| $ddH_2O$ | N/A | 500 mL |
| **Total** | **N/A** | **500 mL** |

*Note:* The ZnO growth solution should be freshly made and stored at 4°C before use.

⚠ CRITICAL: Please pay special attention to the explosive reagents HMTA and $Zn(NO_3)_2 \cdot 6H_2O$.

⚠ CRITICAL: The experimenters should wear protective goggles and rubber gloves to avoid splashing on skin or eyes.

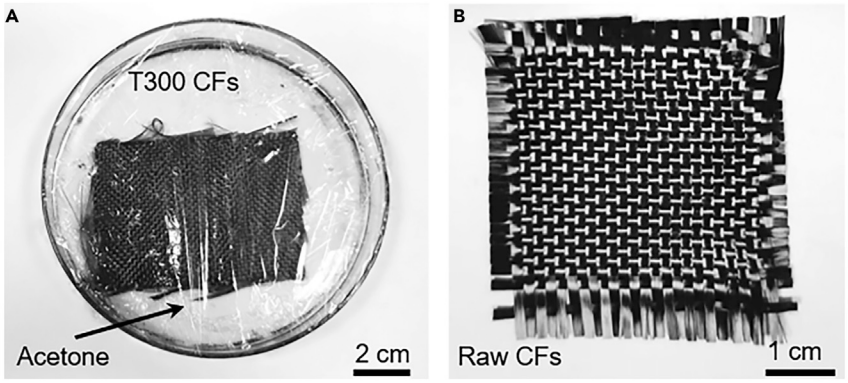


**Figure 3. Raw CFs obtained after desizing in acetone**
(A) Desizing process of commercial CFs in acetone.
(B) Raw CFs after pre-treatment.

## STEP-BY-STEP METHOD DETAILS

### Fiber desizing

Timing: 72 h

1. Fiber desizing procedure.
   a. Remove surface sizing agent and contaminants on the surface of commercial CFs (T300, Toray Ltd., Japan) by soaking in acetone (99.0%, Shanghai Aladdin Biochemical Technology Co., Ltd., China) for 72 h prior to use.
   b. Seale and place the petri dish (Φ 120 mm) with CFs in fume hood during desizing time (Figure 3A).
   c. Ultrasonically clean (KS-800KDE, Kunshan Jielimei Ultrasonic Instrument Co., Ltd., China) for 5–8 min (220 V, 40 KHz, 25°C) and dry at 85°C for 30 min to obtain raw CFs (Figure 3B).

### PDA-CFs preparation

Timing: 7 h

2. PDA solution preparation.
   a. Prepare the aqueous solution of dopamine hydrochloride ($C_8H_{12}ClNO_2$, 1 mg/L) with a final pH of 8.5 by adding tris buffer (30 min).
   b. Added sodium periodate ($NaIO_4$) with the molar ratio to dopamine hydrochloride of 2:1 and stir violently for 30 min (Figures 4A–4C).
   c. $NaIO_4$ as a strong oxidant significantly can short the time of dopamine self-polymerization and accelerate the deposition of poly dopamine on the surface of CFs (Li et al., 2020; Samyn, 2020; Song et al., 2017).
3. PDA-CFs preparation procedure.
   a. Immerse raw CFs completely in the PDA solution for 6 h at room temperature (25°C) (Figure 4D).
   b. Take out the CFs from PDA solution gently.
   c. Ultrasonically clean and dry to obtain PDA-CFs (Figure 4E).

⚠ CRITICAL: Acetone is a toxic reagent and should be used in strict accordance with the specifications.

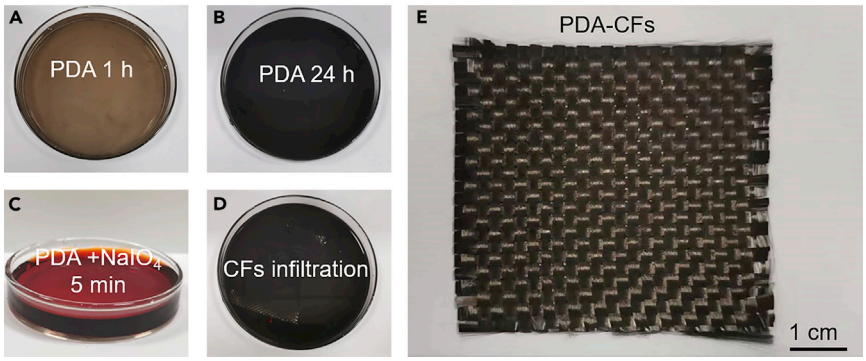


**Figure 4. Self-aggregation of dopamine and prepared PDA-CFs**

(A and B) Dopamine self-aggregation for 1 h and 24 h, respectively.

(C) Dopamine self-aggregation within 5 min after adding $NaIO_4$.

(D) Raw CFs infiltration in PDA solution.

(E) Digital photo of prepared PDA-CFs.

## ZnO seed attachment

Timing: 3 h

4. ZnO seed solution preparation.
   a. Prepare ZnO seed solution (Figures 5A and 5B) by mixing 400 mL 12.5 mM zinc acetate ($Zn(C_2H_3O_2)_2$) in ethanol (99.7%, Shanghai Aladdin Biochemical Technology Co., Ltd., China) solution with 80 mL 20 mM sodium hydroxide in ethanol solution.
   b. Stir the two solutions at 65°C for 30 min.
   c. Dilute the ZnO seed solution to 800 mL by adding ethanol.
   d. Stir the mixed solution continuously for 30 min at 65°C.
   e. Keep the mixed solution at room temperature (25°C) for 1 h after cooling by ice water bath.
5. ZnO seed attachment procedure.
   a. Immerse PDA-CFs completely into the prepared ZnO seed solution for 15 min.
   b. Stir the seed solution evenly to ensure uniform seed synthesis (Figure 5C).
   c. Take out fabrics from ZnO seed solution and anneal in air atmosphere at 150°C for 10 min, then immerse in ZnO seed solution for 15 min (Figure 5D).
   d. Repeat the anneal process for three times.

## ZnO NRs growth

Timing: 7 h

6. ZnO NRs growth solution preparation.
   a. Prepare ZnO growth solution (Figures 6A and 6B) by adding 7.4373 g zinc nitrate hexahydrate ($Zn(NO_3)_2 \cdot 6H_2O$) and 3.5048 g hexamethylenetetramine (HMTA) to 500 mL deionized water (30 min).
   b. Stir the mixed solution evenly at room temperature (25°C) for 30 min to fully dissolve.

⚠ CRITICAL: Please pay special attention to the explosive reagents HMTA and $Zn(NO_3)_2 \cdot 6H_2O$.

7. ZnO NRs growth procedure.
   a. Transfer the prepared ZnO growth solution to a hydrothermal reactor (Figure 6C).

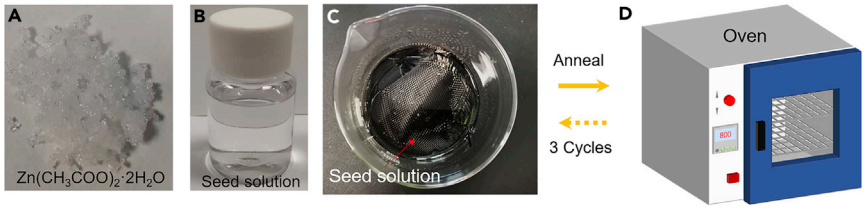


**Figure 5. ZnO seed attachment**

(A and B) Zinc acetate powder and ZnO seed solution.

(C) ZnO seed attached on the surface of PDA-CFs in seed solution.

(D) Anneal in an air oven.

b. Soak PDA-CFs completely into the growth solution at 90°C in the closed thermal reactor for 4 h.

c. Take out fabrics from the hydrothermal reactor.

d. Ultrasonically clean and place the fabrics in a vacuum drying oven at 100°C for 2 h to obtain ZnO-PDA-CFs (Figure 6D).

⚠ CRITICAL: Please pay attention to high temperature during the ZnO NRs preparation process.

## Fabrication of biomimetic carbon fiber composites

Timing: 24–25 h

8. Epoxy solution preparation.
   a. Weigh epoxy resin adhesives A and B according to the mass ratio of 3:1.
   b. Stir adhesive A and B evenly for 5 min to ensure they are fully mixed (Figure 7A).
   c. Extract the residual bubbles in the epoxy resin for 5 min using an evacuating device (Figure 7B).
9. Laminate samples fabrication.
   a. Keep the worktable dry and clean, then release agent (YT-401NC, Kunshan Eituo Composites Co., Ltd, China) as sprayed evenly.
   b. Remove loose fiber bundles from the CFs fabric (Figure 7C).
   c. Place the CFs fabric with epoxy resin layer by layer to form composite preform after the release agent is dried.
   d. Cover the last layer CFs fabric with an area of $S_{CFs}$ with perforated isolation film, adhesive felt and vacuum bag film with areas of $S_1$, $S_2$, $S_3$ in turn, where $S_3 > S_2 > S_1 > S_{CFs}$ (Figures 8A and 8B).
   e. Seal the vacuum bag onto the worktable using a commercial seal tape.
   f. After sealing, vacuum the composite preform to a pressure of 0.1 MPa and cure at room temperature (25°C) for more than 24 h (Figure 8C).

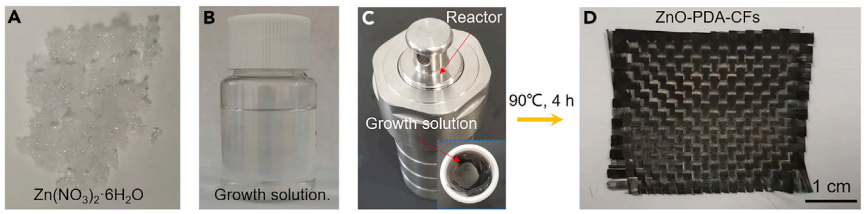


**Figure 6. ZnO NRs preparation process**

(A and B) Zinc nitrate hexahydrate powder and ZnO growth solution.

(C) ZnO NRs growth in a hydrothermal reactor.

(D) Prepared ZnO-PDA-CFs sample.

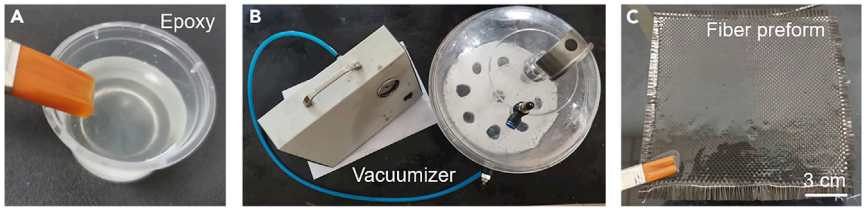


**Figure 7. Preparation and application of epoxy resin**
(A) Epoxy resin preparation.
(B) Bubble extraction setup.
(C) CFs fabric with epoxy resin.

g. Cut the vacuumized composite preform trimly to obtain biomimetic carbon fiber composites.

### Content measurement of PDA, ZnO, EP, and CFs in biomimetic carbon fiber composites

Timing: 1–2 h

In the following steps, the composition proportion of the prepared biomimetic carbon fiber composites will be evaluated.

10. Composition proportion of the biomimetic carbon fiber composites.
    a. Cut each single layer of fabrics with raw CFs, PDA-CFs and ZnO-PDA-CFs into pieces with the size of 2.5 cm×2.5 cm, respectively.
    b. Weigh every five pieces of above single layer to obtain their weight within specific area (2.5 cm×2.5 cm), which are recorded as $W_1$, $W_2$ and $W_3$, respectively.
    c. Fabricate the biomimetic carbon fiber composites as the final products with ZnO-PDA-CFs with above specific size and weighed, which is recorded as $W_4$.
    d. The proportion of each individual composition can be simply calculated as follows: ($W_1$/$W_4$) × 100% (CFs), ($W_2$-$W_1$/$W_4$) × 100% (PDA), ($W_3$-$W_2$/$W_4$) × 100% (ZnO), and ($W_4$-$W_3$/$W_4$) × 100% (EP).

### Comprehensive mechanical tests of biomimetic carbon fiber composites

Timing: 2–3 h

An electrohydraulic universal testing machine (MTS 810) was applied to conduct comprehensive mechanical tests of the biomimetic carbon fiber composites, including tensile, flexural and interlaminar shear tests (Figure 9) (Hu et al., 2020). It should be noted that all the loading rate and sample size were strictly in accordance with the P.R.C. National Testing Standards GB/T 3354-2014 (Sun et al., 2014), GB/T 3356-2014 (Shen et al., 2014) and GB/T 30969-2014 (Xie et al., 2014). All mechanical tests and characterization were performed at room temperature (25°C) and standard humidity (50%–70%). Calculation method of mechanical tests, results statistics and test conditions were introduced in details as follows:

11. Tensile test.
    a. Perform a tensile test in accordance with the P.R.C. National Testing Standards GB/T 3354-2014.
    b. For thin strip style, use the clamping end to clamp and load with friction force at a loading rate of 2 mm/min.

*Note:* Uniform tension field is formed in the style working section.

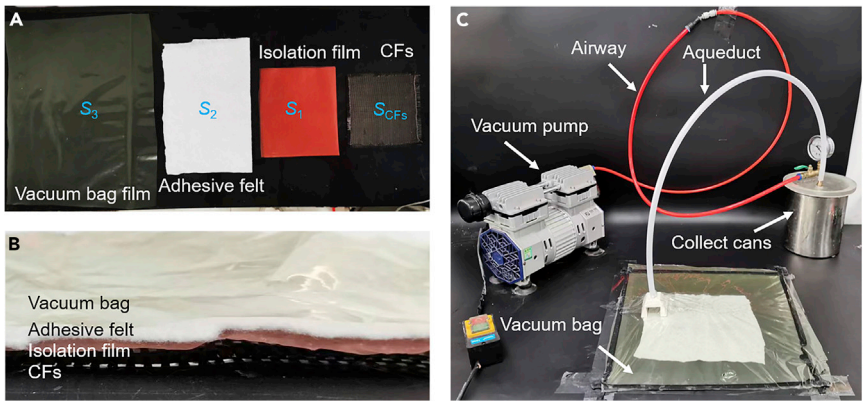


**Figure 8. Key materials used in the fabrication process of biomimetic carbon fiber composites**

(A) Isolation film ($S_1$), adhesive felt ($S_2$), vacuum bag film ($S_3$) and CFs fabric ($S_{CFs}$).

(B) Lay-up sequence of isolation film, adhesive felt and vacuum bag film.

(C) Molding equipment of VACM method.

***Note:*** Tensile strength is calculated by:

$$\sigma_t = \frac{P_{max}}{\omega h} \quad \text{(Equation 1)}$$

$\sigma_t$ —— Tensile strength, (MPa);

$P_{max}$ —— Maximum load before failure, (N);

$\omega$ —— Width of the sample, (mm);

$h$ —— Thickness of the sample, (mm).

***Note:*** Tensile modulus is calculated by:

$$E_t = \frac{\Delta P l}{\omega h \Delta l} \quad \text{(Equation 2)}$$

$E_t$ —— Tensile modulus, (MPa);

$l$ —— The sample length of the working section, (mm);

$\Delta P$ —— Load increment, (N);

$\Delta l$ —— The deformation increment corresponding to $\Delta P$.

⚠ CRITICAL: The length of the sample should be more than 25 cm, the width $\omega$ is $25 \pm 0.1$ mm and the thickness $h$ is 2–4 mm.

12. Flexural test.
    a. Perform a flexural test in accordance with the P.R.C. National Testing Standards GB/T 3356-2014.
    b. For straight strip samples, three-point bending method is used to apply load at a loading rate of 2 mm/min.

***Note:*** The bending stress distribution field is applied in the middle of the sample.

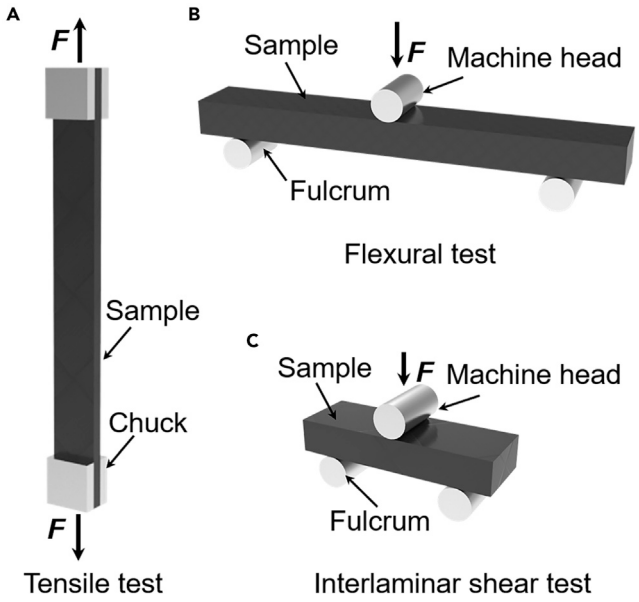


**Figure 9. Schematic diagram of the comprehensive mechanical tests**

(A) Tensile test.

(B) Flexural test.

(C) Interlaminar shear test.

***Note:*** Flexural strength is calculated by:

$$\sigma_f = \frac{3P_{max}L}{2\omega h^2} \quad \text{(Equation 3)}$$

$\sigma_f$ —— Flexural strength, (MPa);

$P_{max}$ —— Maximum load before failure, (N);

$L$ —— Span, (mm);

$\omega$ —— Width of the sample, (mm);

$h$ —— Thickness of the sample, (mm).

***Note:*** Flexural modulus is calculated by:

$$E_f = \frac{\Delta\sigma}{\Delta\varepsilon} \quad \text{(Equation 4)}$$

$E_f$ —— Flexural modulus, (MPa);

$\Delta\sigma$ —— The difference of bending stresses between two selected strain points, (MPa);

$\Delta\varepsilon$ —— The difference of bending strains between two selected strain points, (mm/mm).

⚠ CRITICAL: The length of the sample should be more than ($L$+20) mm, the width $\omega$ is 25 $\pm$ 0.1 mm, the thickness $h$ is 2–4 mm and $L = 32h$.

13. Interlaminar shear test.

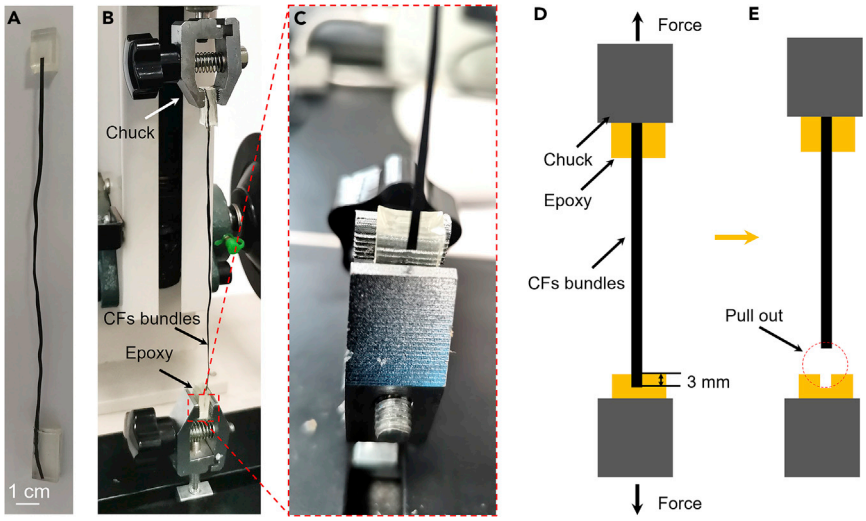


**Figure 10. Qualitative test of interface strength**
(A) Fiber bundle with both ends fixed.
(B) Test apparatus.
(C) Sample clamped position.
(D and E) Diagram of interface strength qualitative test.

a. Perform a flexural test in accordance with the P.R.C. National Testing Standards GB/T 30969-2014.
b. For straight strip samples, three-point bending method is used to apply load at a loading rate of 2 mm/min.

***Note:*** The bending stress distribution field is applied in the middle of the sample.

***Note:*** ILSS is calculated by:

$$\tau_{sbs} = \frac{3P_{max}}{4\omega h} \quad \text{(Equation 5)}$$

$\tau_{sbs}$ —— ILSS, (MPa);

$P_{max}$ —— Maximum load before failure, (N);

$\omega$ —— Width of the sample, (mm);

$h$ —— Thickness of the sample, (mm).

***Note:*** Generally, interlaminar shear modulus is calculated by:

$$E_{sbs} = 0.425E_f \quad \text{(Equation 6)}$$

$E_{sbs}$ —— Interlaminar shear modulus, (MPa);

$E_f$ —— Flexural modulus of short beam under three points bending, (MPa).

⚠ CRITICAL: The length of the sample should be more than (5$h$+10) mm, the thickness $h$ is 2–6 mm and the width $\omega$ = 2–3$h$.

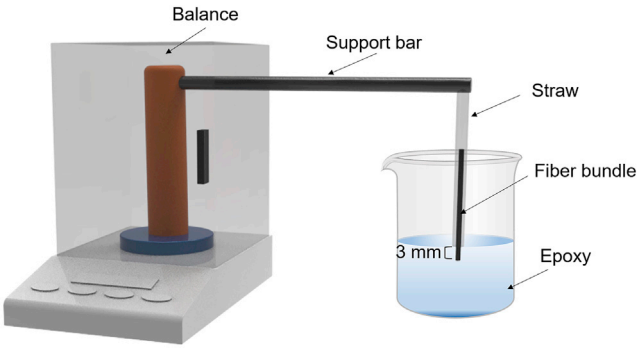


**Figure 11. Schematic diagram of RIC test**
Published in Wang et al. (2022).

## Qualitative test of interface strength

Timing: 1–2 h

14. Interface strength between fibers and epoxy.
    a. Precure epoxy resin in rubber mold.
    b. Cut a bundle of raw CFs, PDA-CFs and ZnO-PDA-CFs with equal length, respectively.
    c. The fiber axis of the bundle should perpendicular to the epoxy resin level.

    *Note:* Soak one end of the bundle in the precured epoxy resin by 3 mm.

    d. Another end of the bundle is dipped into the epoxy resin with a length greater than 3 mm.
    e. After curing, tight both ends of the bundle.

    *Note:* Keep the fiber axis the same direction as the load force.

    f. Applied the load uniformly to pull the bundle out of the epoxy resin (Figure 10).

    *Note:* At least five bundles of each sample were used for interface strength test, respectively.

## Resin infiltration capacity (RIC) test

Timing: 1–2 h

15. RIC tests of fiber bundles (Figure 11).
    a. Fill raw CFs and modified CFs (PDA-CFs and ZnO-PDA-CFs) into a straw with a diameter of about 3 mm and a filling rate of 47%–53%.

    *Note:* The length of fibers exposed from the straw should be about 3 mm.

    b. Suspend the straw vertically from the support bar.
    c. Place the entire test rack on the analytical balance (BSA224S, Sartorius).
    d. Dip the straw end into the epoxy resin vertically.
    e. Keep fiber bundle in contact with the epoxy resin surface, which makes it rise along the fiber gap due to capillarity.
    f. Record the mass changes shown by the analytical balance over time.

*Note:* In the process of epoxy resin infiltration, the mass of the fibers will gradually increase until reached a stable value.

g. Record the data per second until the mass changes are no longer noticeable.

*Note:* Use at least five bundles of each sample for RIC tests, respectively.

## EXPECTED OUTCOMES

The prepared ZnO NRs have good uniformity. The diameter of most counted ZnO NRs was 0.26–0.32 μm and the length was 1.1–1.5 μm (Figure 12A). The element proportion of C, Zn, and O was 50.76 wt %, 31.90 wt %, and 17.33 wt %, respectively (Figure 12B). It provided the preliminary evidence that dense ZnO NRs successfully grew on the surface of the PDA-CFs. FTIR spectra of the three kinds of samples with pre-modification and post-modification were obtained (Figure 12C). For raw CFs, characteristic peak at 1610 $cm^{-1}$ was found, which belonged to aromatic C-C stretching vibration. N-H shearing vibration peak appeared at 1,480 $cm^{-1}$–1,560 $cm^{-1}$ in PDA-CFs and ZnO-PDA-CFs. The peak at 1,589 $cm^{-1}$ can be attributed to the stretching vibration of benzene ring in PDA-CFs, which moved to 1,635 $cm^{-1}$ after the growth of ZnO NRs. The shift of these peaks also indicated that the coordination between $Zn^{2+}$ and PDA took place. Both samples had a broad peak near 3,400 $cm^{-1}$, which was caused by the stretching vibrations of functional groups like -$NH_2$, -NH-, and -OH in PDA. In addition, XRD spectra (Figure 12D) showed that there were two peaks at 26° and 42°of the raw CFs and PDA-CFs, which belonged to C (002) and C (10). In contrast, many new diffraction peaks appeared in the ZnO-PDA-CFs, which were at 31.6° (100), 34.3° (002), 36.5° (101), 47.5° (102), 56.5°(110), 62.4° (103), 66.1° (200), and 68.5° (112). When compared to raw CFs and PDA-CFs, ZnO-PDA-CFs demonstrated the strongest bond strength with a peak load of 22.52±3.15 N (Figure 12E). For the qualitative test of interface strength, the peak load of ZnO-PDA-CFs increased by 98.94% and 41.28% than that of raw CFs (11.32±1.39 N) and PDA-CFs (15.94±1.07 N), respectively. For the RIC test, the final RIC of raw CFs was 11.64±1.10 mg, while the RIC of PDA-CFs increased by 24.57% and reached to 14.50±0.52 mg. Similarly, when compared to PDA-CFs, the RIC of ZnO-PDA-CFs was 17.54±0.38 mg, which increased by 20.97% (Figure 12F). Compared to many other conventional modification methods, such as coating, surface oxidation, nanofiller or grafting (Prakash and Rajadurai, 2017; He et al., 2021; Dai et al., 2011; Andideh and Esfandeh, 2016; Wang et al., 2019; Chukov et al., 2019; Sun et al., 2020; Sepe et al., 2018; Nie et al., 2017; Hu et al., 2018; Huan et al., 2020; Zhu et al., 2017; Zhang et al., 2020; Fu et al., 2019), the improved mechanical performance as well as other foreseeable advantages of the proposed two-step modification method are considerable (Figure 13).

## LIMITATIONS

Due to the limited resources of wing feathers, this work only explored the HGMS of Black Kite (*Milvus migrans*). More wing feathers of typical raptors with elaborated structures can also be comparatively investigated to figure out the universal interlocking mechanism. The biomimetic design strategy was proved to be effective to innovate the fabrication process of traditional carbon fiber composites under laboratory conditions, while the feasibility of rapid scale-up needs to be further verified.

## TROUBLESHOOTING

### Problem 1

The current molding method was suitable for laboratory research, but improved molding methods need to be further explored for mass production of large-scale samples (fabrication of biomimetic carbon fiber composites, step 9).

### Potential solution

Compression molding and resin transfer molding (RTM) are suitable for large-scale sample molding with high mechanization and production efficiency.

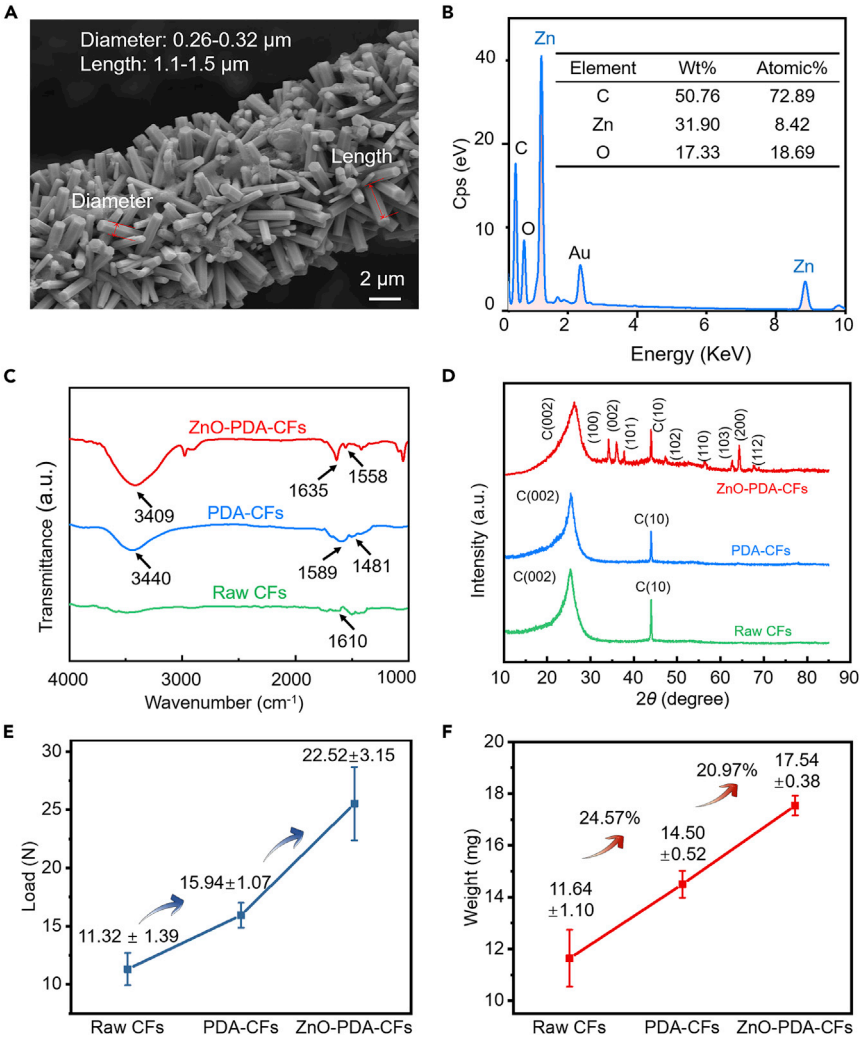


**Figure 12. Expected outcomes**

(A) Geometric dimension statistics of ZnO NRs.

(B) Element proportion of C, Zn, and O from ZnO-PDA-CFs. The element proportion of C, Zn, and O was 50.76 wt %, 31.90 wt %, and 17.33 wt %. Published in Wang et al. (2022).

(C) FTIR spectra of raw CFs, PDA-CFs, and ZnO-PDA-CFs demonstrating clear peak changes. Published in Wang et al. (2022).

(D) XRD spectra of raw CFs, PDA-CFs, and ZnO-PDA-CFs for peak comparison. Typical diffraction peaks of hexagonal wurtzite structure of ZnO can be found in the ZnO-PDA-CFs. Published in Wang et al. (2022).

(E) Qualitative test of interface strength. Published in Wang et al. (2022).

(F) RIC comparison of raw CFs, PDA-CFs and ZnO-PDA-CFs. Published in Wang et al. (2022).

## Problem 2

Interfacial reinforcement effect of ZnO NRs towards composite liminates was comfirmed in this case. However, the impacts of the geometric parameters of ZnO NRs on the interfacial strength between CFs and epoxy resin were not clear (qualitative test of interface strength, step 14).

## Potential solution

It was preliminarily found that the geometric size of ZnO NRs was related to the attachment and annealing times of ZnO seed as well as the growth time of ZnO NRs in growth solution.

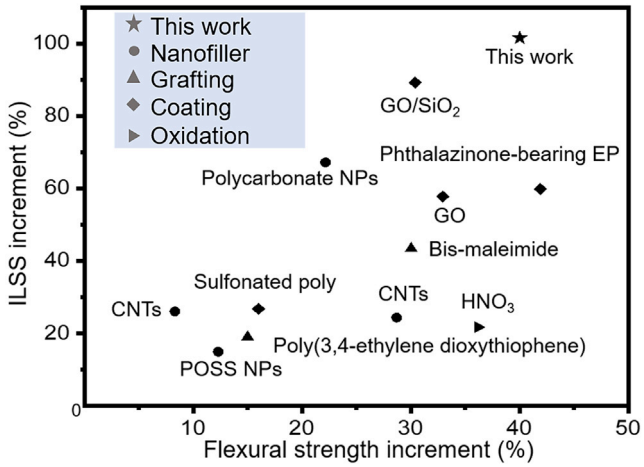


**Figure 13. Comparison of enhancement effects on flexural strength and ILSS via different modification methods**
Published in Wang et al. (2022).

### Problem 3

In addition to the qualitative tear resistance test, the enhancement effect of HGMS in wing feathers also needs data support (characterization and interlocking mechanism of natural HGMS, before you begin).

### Potential solution

The maximum separation force and damage resistance of the wing feathers with HGMS can be quantitatively measured with a micro tension meter.

### Problem 4

From the perspective of experimental results, the enhancement effect and mechanism of bioinspired design strategy was comprehensively analyzed, but the theoretical depth was insufficient (comprehensive mechanical tests of biomimetic carbon fiber composites, step 11, 12, 13).

### Potential solution

Systematic mechanics modeling was a considerable option for failure analysis, which could further enhance the theoretical depth of this work.

### Problem 5

The bioinspired design strategy proposed in this study has significant enhancement effect on carbon fiber/E51 epoxy plate parts, but the enhancement effect for curved parts of other fiber types still needs to be studied (fabrication of biomimetic carbon fiber composites, step 9).

### Potential solution

Different kinds of fiber (glass fiber, aramid fiber, etc.) and resin systems (phenolic resin, unsaturated polyester resin, etc.) can be used to prepare curved surface samples by molding or RTM to explore the enhancement effect of bioinspired design strategy.

## RESOURCE AVAILABILITY

### Lead contact

Further information and requests for resources and reagents should be directed to and will be fulfilled by the lead contact, Zhengzhi Mu (zmu@jlu.edu.cn).

### Materials availability

This study did not generate new unique reagents.

### Data and code availability

All data reported in this paper will be shared by the lead contact upon request.

This paper does not report original code.

Any additional information required to reanalyze the data reported in this paper is available from the lead contact upon request.

## ACKNOWLEDGMENTS

The work was financially supported by the National Key Research and Development Program of China (No. 2018YFA0703300), the Foundation for Innovative Research Groups of the National Natural Science Foundation of China (No. 52021003), the National Natural Science Foundation of China (Nos. 51835006, and 52105298), National Postdoctoral Program for Innovative Talents (No. BX20190139), China Postdoctoral Science Foundation (Nos. 2020M670844 and 2021M701386).

## AUTHOR CONTRIBUTIONS

Conceptualization, Y.W., Z.M., and Z.H.; Methodology, Y.W. and Z.M.; Investigation, W.S., Z.Z., and Z.W.; Writing – Original Draft, Y.W. and Z.M.; Writing – Review & Editing, Y.W. and Z.M.; Funding Acquisition, Z.M., Z.H., and L.R.; Resources, Z.M., Z.H., and L.R.; Supervision, Z.M., Z.H., and L.R.

## DECLARATION OF INTERESTS

The authors declare no competing interests.

## REFERENCES

Andideh, M., and Esfandeh, M. (2016). Statistical optimization of treatment conditions for the electrochemical oxidation of PAN-based carbon fiber by response surface methodology: application to carbon fiber/epoxy composite. Compos. Sci. Technol. *134*, 132–143.

Chukov, D., Nematulloev, S., Torokhov, V., Stepashkin, A., Sherif, G., and Tcherdyntsev, V. (2019). Effect of carbon fiber surface modification on their interfacial interaction with polysulfone. Results Phys. *15*, 102634.

Dai, Z., Zhang, B., Shi, F., Li, M., Zhang, Z., and Gu, Y. (2011). Effect of heat treatment on carbon fiber surface properties and fibers/epoxy interfacial adhesion. Appl. Surf. Sci. *257*, 8457–8461.

Fu, J., Zhang, M., Jin, L., Liu, L., Li, N., Shang, L., Li, M., Xiao, L., and Ao, Y. (2019). Enhancing interfacial properties of carbon fibers reinforced epoxy composites via layer-by-layer self assembly GO/$SiO_2$ multilayers films on carbon fibers surface. Appl. Surf. Sci. *470*, 543–554.

He, H., Zhang, T., and Yang, Y. (2021). A facile way to modify carbon fibers and its effect on mechanical properties of epoxy composites. J. Mater. Res. Technol. *10*, 164–174.

Hu, J., Li, F., Wang, B., Zhang, H., Ji, C., Wang, S., and Zhou, Z. (2020). A two-step combination strategy for significantly enhancing the interfacial adhesion of CF/PPS composites: the liquid-phase oxidation followed by grafting of silane coupling agent. Compos. B Eng. *191*, 107966.

Hu, Z., Shao, Q., Huang, Y., Yu, L., Zhang, D., Xu, X., Lin, J., Liu, H., and Guo, Z. (2018). Light triggered interfacial damage self-healing of poly (p-phenylene benzobisoxazole) fiber composites. Nanotechnology *29*, 185602.

Huan, X., Shi, K., Yan, J., Lin, S., Li, Y., Jia, X., and Yang, X. (2020). High performance epoxy composites prepared using recycled short carbon fiber with enhanced dispersibility and interfacial bonding through polydopamine surface-modification. Compos. B Eng. *193*, 107987.

Li, B., Luo, J., Huang, X., Lin, L., Wang, L., Hu, M., Tang, L., Xue, H., Gao, J., and Mai, Y.W. (2020). A highly stretchable, super-hydrophobic strain sensor based on polydopamine and graphene reinforced nanofiber composite for human motion monitoring. Compos. B Eng. *181*, 107580.

Nie, C., Yang, Y., Cheng, C., Ma, L., Deng, J., Wang, L., and Zhao, C. (2017). Bioinspired and biocompatible carbon nanotube-Ag nanohybrid coatings for robust antibacterial applications. Acta Biomater. *51*, 479–494.

Prakash, V.R.A., and Rajadurai, A. (2017). Inter laminar shear strength behavior of acid, base and silane treated E-glass fibre epoxy resin composites on drilling process. Defence Technol. *13*, 40–46.

Samyn, P. (2020). Engineering the cellulose fiber interface in a polymer composite by mussel-inspired adhesive nanoparticles with intrinsic stress-sensitive responsivity. ACS Appl. Mater. Interfaces *12*, 28819–28830.

Sepe, R., Bollino, F., Boccarusso, L., and Caputo, F. (2018). Influence of chemical treatments on mechanical properties of hemp fiber reinforced composites. Compos. B Eng. *133*, 210–217.

Shen, W., Yang, S.C., Shen, Z., Zhang, Z.L., Wang, L.P., Wang, H.P., Wang, J., and Quan, C.X. (2014). Test Method for Flexural Properties of Orientational Fiber Reinforced Polymer Metrix Composite Materials (Standardization Administration of the P.R.C). GB/T 3356-2014.

Song, P., Xu, Z., Dargusch, M.S., Chen, Z., Wang, H., and Guo, Q. (2017). Granular nanostructure: a facile biomimetic strategy for the design of supertough polymeric materials with high ductility and strength. Adv. Mater. *29*, 1704661.

Sun, J.S., Yang, S.C., Shen, Z., Chen, X.W., Wang, X.H., Shen, W., Wang, J., and Xiao, J. (2014). Test Method for Tensile Properties of Orientation Fiber Reinforced Polymer Matrix Composite Materials (Standardization Administration of the P.R.C). GB/T 3354-2014.

Sun, Y., Yang, C., and Lu, Y. (2020). Weak layer exfoliation and an attempt for modification in anodic oxidation of PAN-based carbon fiber. J. Mater. Sci. *55*, 2372–2379.

Wang, D., Bai, T., Cheng, W., Xu, C., Wang, G., Cheng, H., and Han, G. (2019). Surface modification of bamboo fibers to enhance the interfacial adhesion of epoxy resin-based composites prepared by resin transfer molding. Polymers *11*, 2107.

Wang, Y., Mu, Z., Zhang, Z., Song, W., Zhang, S., Hu, H., Ma, Z., Huang, L., Zhang, D., Wang, Z., et al. (2022). Interfacial reinforced carbon fiber composites inspired by biological interlocking structure. iScience *25*, 104066.

Xie, J.H., Yang, S.C., Shen, Z., Shen, W., Li, X.Q., Sun, J.S., Zhou, J.F., and Xiao, J. (2014). Test Method for Short-Beam Shear Strength of Polymer Matrix Composite Materials (Standardization Administration of the P.R.C). GB/T 30969-2014.

Zhang, M., Ding, L., Zheng, J., Liu, L., Alsulami, H., Kutbi, M.A., and Xu, J. (2020). Surface modification of carbon fibers with hydrophilic Fe3O4 nanoparticles for nickel-based multifunctional composites. Appl. Surf. Sci. *509*, 145348.

Zhu, J., Yuan, L., Guan, Q., Liang, G., and Gu, A. (2017). A novel strategy of fabricating high performance UV-resistant aramid fibers with simultaneously improved surface activity, thermal and mechanical properties through building polydopamine and graphene oxide bi-layer coatings. Chem. Eng. J. *310*, 134–147.